Biosensors and Bioelectronics 94 (2017) 433–437

Contents lists available at ScienceDirect

Biosensors and Bioelectronics

journal homepage: www.elsevier.com/locate/bios

A novel versatile microbiosensor for local hydrogen detection by means of scanning photoelectrochemical microscopy

Fangyuan Zhao[a,1], Felipe Conzuelo[a,1], Volker Hartmann[b], Huaiguang Li[c], Stefanie Stapf[c], Marc M. Nowaczyk[b], Matthias Rögner[b], Nicolas Plumeré[c], Wolfgang Lubitz[d], Wolfgang Schuhmann[a,*]

[a] Analytical Chemistry – Center for Electrochemical Sciences (CES), Ruhr-Universität Bochum, Universitätsstr. 150, D-44780 Bochum, Germany
[b] Plant Biochemistry, Ruhr-Universität Bochum, Universitätsstr. 150, D-44780 Bochum, Germany
[c] Center for Electrochemical Sciences – Molecular Nanostructures, Ruhr-Universität Bochum, Universitätsstr. 150, D-44780 Bochum, Germany
[d] Max Planck Institut für Chemische Energiekonversion, Stiftstrasse 34-36, D-45470 Mülheim an der Ruhr, Germany

ARTICLE INFO

Keywords:
Hydrogenase
Viologen-modified redox polymer
Oxygen-protection shield
SECM
Hydrogen biosensor
PS1-Pt

ABSTRACT

The development of a versatile microbiosensor for hydrogen detection is reported. Carbon-based microelectrodes were modified with a [NiFe]-hydrogenase embedded in a viologen-modified redox hydrogel for the fabrication of a sensitive hydrogen biosensor By integrating the microbiosensor in a scanning photoelectrochemical microscope, it was capable of serving simultaneously as local light source to initiate photo(bio) electrochemical reactions while acting as sensitive biosensor for the detection of hydrogen. A hydrogen evolution biocatalyst based on photosystem 1-platinum nanoparticle biocomplexes embedded into a specifically designed redox polymer was used as a model for proving the capability of the developed hydrogen biosensor for the detection of hydrogen upon localized illumination. The versatility and sensitivity of the proposed microbiosensor as probe tip allows simplification of the set-up used for the evaluation of complex electrochemical processes and the rapid investigation of local photoelectrocatalytic activity of biocatalysts towards light-induced hydrogen evolution.

1. Introduction

The global demand for energy sources that can satisfy the need of an ever-growing population and the adverse consequences for the environment originating from burning of fossil fuels have turned to the development of an economy using more efficient, clean and renewable energy sources. The increasing interest for a hydrogen-based economy and possible replacement of traditional fossil fuels requires the development of a sustainable hydrogen production. In this regard, particular interest is directed towards the search and development of catalysts or biocatalysts capable of performing hydrogen evolution from water (Krassen et al., 2011; Reisner, 2011; Vesborg et al., 2015; Zheng et al., 2014). Fast and reliable methods are required to assess the activity of (photo)catalysts for the hydrogen evolution reaction (HER).

Of particular interest in the evaluation of catalytic materials is the laterally-resolved characterization of a surface in search for local active hot-spots for catalysis. This allows the study of heterogeneous samples and materials libraries in search of a highly active material with a particular composition. Scanning electrochemical microscopy (SECM) allows studying the local electrochemical or electrocatalytic properties of a surface. By recording the current obtained at an accurately positioned SECM tip electrode as function of tip location, chemical images are obtained, which translate to differences in reaction rates at different locations at the surface. SECM has found wide application in different fields, among them, the measurements of local heterogeneous reaction kinetics, homogeneous kinetics and the investigation of bioctalytic systems (Amemiya et al., 2008; Edwards et al., 2006; Sun et al., 2007). The further demand for exploring new materials and complex catalytically active surfaces requires the development of new methodologies on the basis of SECM principles (Bertoncello, 2010; Cannan et al., 2011; Zoski, 2015). Local detection of hydrogen evolution using SECM has been reported for the evaluation of the electrocatalytic activity of electrocatalysts (Jamali et al., 2015; Jedraszko et al., 2014) or the corrosion of metals (Tefashe et al., 2014). Further improvement was made recently by implementing a

* Corresponding author.
E-mail address: wolfgang.schuhmann@rub.de (W. Schuhmann).
[1] F. Z. and F. C. contributed equally to this work.

http://dx.doi.org/10.1016/j.bios.2017.03.037
Received 16 December 2016; Received in revised form 15 March 2017; Accepted 17 March 2017
Available online 18 March 2017
0956-5663/

scanning photoelectrochemical microscopy (SPECM) set-up that allows high-resolution visualization of the photoactivity of semiconductors as well as photoactive protein complexes such as photosystem 1 (PS1) and photosystem 2 (PS2) under controlled and localized irradiation conditions (Zhao et al., 2015; Conzuelo et al., 2017). A Pt microelectrode was used for the collection of biophotocatalytically evolved hydrogen which showed limited sensitivity when smaller electrode tips are used for the high resolution analysis of a given surface. In addition, the use of unmodified electrode surfaces and the necessary relatively high applied potential for hydrogen detection make this approach prone to the influence of interfering compounds.

Enzyme-based biosensors play an important role in the determination of a number of molecules of interest due to their inherent sensitivity and especially high selectivity. Moreover, their unique features such as high efficiency at mild pH values and temperature conditions, rapid response and capability of miniaturization make them an attractive tool for the analysis and continuous monitoring of a variety of different analytes (Sassolas et al., 2012). Hydrogenases (H_2ases) are nature's efficient biocatalysts for the reversible $H_2/2H^+$ interconversion at high turnover rates and low overpotentials. However, the application of hydrogenases in biosensors has been limited so far, since the enzymes suffer from deactivation by both oxygen and high applied potentials (Lubitz et al., 2014). Recently, we have proposed an elegant method to overcome these limitations and to shield hydrogenases from both deactivation by molecular oxygen as well as high applied potentials (Plumeré et al., 2014). By integrating a [NiFe]-hydrogenase within a viologen-based redox hydrogel, an efficient bioelectrode for H_2 oxidation was achieved even in the presence of high concentrations of oxygen. Further work evaluated the protective role of the viologen-based redox polymer from oxygen and high potentials (for a detailed description, the reader is referred to: Fourmond et al., 2015) and allowed the successful protection of the enzyme when replacing a [NiFe]-hydrogenase by an [FeFe]-hydrogenase which is usually irreversibly deactivated by oxygen (Oughli et al., 2015). These results open up a new possibility for the development of hydrogenase-based hydrogen biosensors.

We present a hydrogenase/viologen-based redox hydrogel modified microelectrode integrated into a scanning photoelectrochemical microscopy (SPECM) set-up using the hydrogen biosensor simultaneously as light source for local illumination as well as for the localized determination of photocatalytically evolved hydrogen. To demonstrate the ability of the developed hydrogen microbiosensor to locally detect (bio) photocatalytically generated hydrogen, a gold surface modified with a composite of photosystem 1/Pt nanoparticle biocomplexes (PS1-Pt) embedded in an Os-complex modified redox polymer was selected (Zhao et al., 2015). By polarizing the PS1-Pt/redox polymer modified Au surface at a suitable potential for light-induced hydrogen evolution, variations in the hydrogen production rate were successfully visualized by scanning the developed hydrogen microbiosensor across the sample in the sample generation/tip collection mode of SECM.

2. Materials and methods

2.1. Reagents and chemicals

Citric acid monohydrate, sodium phosphate and potassium chloride were from J.T. Baker. Tris(hydroxymethyl)aminomethane-HCl (Tris–HCl) was from AppliChem. Poly(ethyleneglycol)diglycidyl ether (PEGDGE) was from Polysciences. Hexaammineruthenium (III) chloride was from Sigma-Aldrich. All chemicals were of analytical grade and used without further purification. All solutions were prepared using deionized water (ρ=18 MΩ cm). The viologen-functionalized polyethylenimine polymer was synthesized as described elsewhere (Plumeré et al., 2014). [NiFe]-hydrogenase from *Desulfovibrio vulgaris* Miyazaki F (*Dv*MF [NiFe]-H_2ase) was obtained and purified as described previously (Fichtner et al., 2006; Yagi et al., 1976). The poly(1-vinylimidazole-*co*-allylamine) polymer modified with $[Os(bpy)_2Cl]^+$ was synthesized as described earlier (Badura et al., 2008; Sokol et al., 2016). PS1-Pt bioconjugates were prepared as described in (Zhao et al., 2015). Briefly, freshly synthesized mercaptosuccinic acid-stabilized Pt nanoparticles were coupled to PS1 extracted from *Thermosyne chococcus elongatus* (Badura et al., 2011) by incubating overnight in the dark at 4 °C. The self-assembled PS1-Pt complexes were purified by microfiltration in order to remove unbound Pt nanoparticles.

2.2. Preparation of hydrogenase-modified microelectrodes

Carbon microelectrodes were prepared using a modified procedure for the preparation of carbon nanoelectrodes (Clausmeyer et al., 2014). Quartz capillaries (Sutter Instruments; outer diameter 1.2 mm, inner diameter 0.9 mm) were pulled using a P-2000 laser puller (Sutter Instruments) to obtain fine tips. A dense layer of carbon was deposited on the inner wall of the pulled capillaries by pyrolysis of a butane/propane (80/20) mixture heated under inert atmosphere (Ar). The tips were then polished on polishing paper of different grain sizes until an opening of desired dimensions was obtained. Then, the tip of the prepared microelectrode was sealed with carbon paste (Leit-C, Plano), removing the excess deposited on the sheath of the capillary. A copper wire coated with silver cement (Leitsilber, Plano) was inserted into the opposite end of the capillary for electrical connection. The prepared carbon microelectrodes were carefully polished and characterized by recording cyclic voltammograms in 5 mM $[Ru(NH_3)_6]Cl_3$ containing 0.1 M KCl. A typical steady-state cyclic voltammogram for disk-shaped microelectrodes was obtained with calculated dimensions of 18–20 µm in diameter. These carbon microelectrodes were used as basis for the fabrication of hydrogenase-based microbiosensors. For this, the tip of the carbon microelectrode was inserted into a mixture of *Dv*MF [NiFe]-hydrogenase (35 µM) and the viologen-based polymer (10 µg $µL^{-1}$) and incubated overnight at 4 °C. The obtained modified microelectrode is schematically depicted in Fig. 1. Carbon fiber electrodes prepared as described elsewhere (Schulte and Chow, 1996) were also used as electrodes for the fabrication of similar hydrogen microbiosensors for comparison.

2.3. Cyclic voltammetry

Cyclic voltammograms were recorded with an Autolab PGSTAT30 potentiostat (Metrohm-Autolab) using a three-electrode system comprising the hydrogen biosensor as working electrode, a miniaturized Ag/AgCl/3 M KCl as reference electrode and a Pt wire as counter electrode. All potentials are referred to the Ag/AgCl/3 M KCl reference electrode.

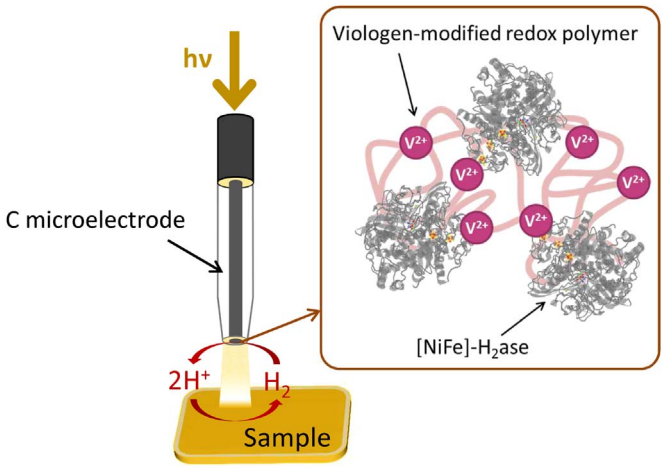

Fig. 1. Schematic representation of the [NiFe]-hydrogenase/viologen-based polymer modified hydrogen microbiosensor used as SPECM tip.

2.4. Calibration of the hydrogen microbiosensor

The hydrogen microbiosensor, the reference and counter electrodes were placed in an electrochemical cell containing 0.1 M phosphate buffer solution of pH 7.0 at (25 ± 2) °C. The cell was bubbled with argon for about 30 min to completely remove dissolved oxygen. The chronoamperometric response of the microbiosensor was recorded at an applied potential of 0 mV (vs. Ag/AgCl/3 M KCl) using a CHI 1030 multipotentiostat. After a stable baseline of the recorded current was obtained, different amounts of hydrogen were added to the cell to adjust increasing hydrogen partial pressure in the buffer solution. For this, a hydrogen/argon mixed feed was bubbled into the electrolyte solution until a constant pressure was reached, which was controlled by means of a Bunsen valve incorporated into the otherwise sealed electrochemical cell. By adjusting the argon to hydrogen ratio in the mixed gas feed and assuming Henry's law the concentration of the dissolved gas was calculated as a basis for the calibration curve.

2.5. Preparation of PS1-Pt samples

Au-coated Si(100) wafers (Wacker) prepared by vapor deposition of a titanium adhesion layer (50 Å) and a 1000 Å gold layer were used for the deposition of PS1-Pt samples. After cleaning with Piranha solution and rinsing with water, modification was done by drop-casting with a mixture of PS1-Pt, PEGDGE and the Os-complex-modified redox polymer followed by incubation overnight in the dark at 4 °C. Prior to the measurement, the samples were immersed for 30 min in 50 mM Tris–HCl buffer pH 9.0 containing 100 mM KCl, 10 mM $MgCl_2$, and 10 mM $CaCl_2$ to induce polymer collapse and crosslinking (Kothe et al., 2014).

2.6. Scanning photoelectrochemical microscopy measurements

SPECM measurements were performed using a set-up (Conzuelo et al., 2017) consisting of three step-motor driven micrometer screws (Owis) for positioning of the microbiosensor in all three spatial directions, a bipotentiostat (PGU-BI 100, IPS-Jaissle), and a control software. A Xe-Hg lamp (LC8 type 03, Hamamatsu Photonics) was coupled with the top glass wall of the microbiosensor by means of a light fiber (HITRONIC POF Simplex PE) for local illumination of the sample. Measurements were performed in a four-electrode configuration consisting of the PS1-Pt modified Au surface, the H_2ase/viologen polymer-modified microbiosensor, a miniaturized Ag/AgCl/3 M KCl reference electrode, and a cylindrical Pt mesh counter electrode.

The microbiosensor was precisely positioned above the PS1-Pt modified sample by recording SECM z-approach curves at three different x,y-positions for automatic tilt correction during area scans. After bubbling the solution with Ar, area scans were recorded under dark and local illumination at a tip-to-sample distance of 10 µm. The tip potential was held at 0 mV vs. Ag/AgCl/3 M KCl allowing the detection of locally evolved hydrogen (see Fig. 1).

3. Results and discussion

3.1. Electrochemical characterization of the hydrogen microbiosensor

The catalytic properties of the microelectrodes modified with [NiFe]-H_2ase embedded in the viologen-based redox hydrogel were investigated by recording cyclic voltammograms in phosphate buffer solution at pH 7.0 saturated with argon or a mixture of hydrogen and argon. As shown in Fig. 2, nearly symmetrical cathodic and anodic redox peaks were observed under argon with a small peak separation of about 30 mV indicating a surface-confined electrochemical process. This confirmed the presence of the viologen-modified redox polymer on the surface of the microelectrode and fast electron transfer kinetics within the redox hydrogel film. Upon bubbling of the solution with a mixed feed of 95% argon and 5% hydrogen a typical catalytic current for hydrogen oxidation was observed (Fig. 2).

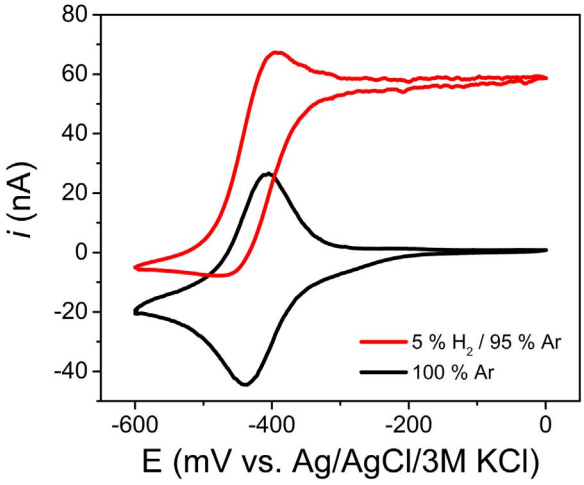

Fig. 2. Cyclic voltammograms for a *Dv*MF [NiFe]-H_2ase/viologen polymer modified microbiosensor recorded in the presence and absence of H_2. Electrolyte: 0.1 M phosphate buffer, pH 7.0. Scan rate: 10 mV s^{-1}.

The increase in anodic current occurs due to hydrogen oxidation by the H_2ase which transfers the electrons to the polymer-bound viologen moieties under formation of the respective radical cations. An electron hopping process is established between adjacent viologen centers in the redox polymer, allowing for electron transfer to the electrode surface at sufficiently high applied anodic potentials at the microbiosensor. The polymer-bound viologen centers are solely responsible for electron transfer between the electrode and the polymer-entrapped hydrogenase as demonstrated by the catalytic wave for hydrogen oxidation, which is centered at the formal potential of the viologen redox couple. Moreover, the shape of the catalytic wave confirmed the protective effect of the polymer from deactivation of the hydrogenase by high applied potentials (Fourmond et al., 2015; Oughli et al., 2015; Plumeré et al., 2014).

The versatility of the fabrication of hydrogen microbiosensors was proved by successfully modifying microelectrodes of different diameters. For comparison, carbon fiber microelectrodes with diameters of 6–8 µm were modified with the H_2ase/viologen polymer, providing a similar response towards the presence of hydrogen in solution (Fig. 3A). Miniaturization of the biosensor is important aiming at a high resolution analysis of (bio)catalytic surfaces. However, the very low amount of enzyme immobilized on the inherently small surface area of these kind of electrodes was leading to very small catalytic hydrogen oxidation currents. Thus, if a higher sensitivity is required, the surface area of the biosensor needs to be increased providing the basis for the immobilization of a higher amount of the H_2ase. As an example for this approach, we prepared a carbon paste-based microelectrode with an increased surface capable to provide a larger current response (see Fig. 3B; cf. with Fig. 2).

Comparison of cyclic voltammograms for the different H_2ase/viologen polymer modified microelectrodes in absence and presence of hydrogen in solution showed their capability of acting as an effective hydrogen biosensor in all cases (Figs. 2 and 3). Since smaller sensors did not provide sufficient H_2 detection capability when analyzing the selected samples based on PS1-Pt nanoparticle biocomplexes, microelectrodes with a diameter between 18 and 20 µm were selected as a compromise between detection limit and sensitivity on the one hand and the size-dependent lateral resolution on the other hand. The sensitivity in the detection of hydrogen was further evaluated by recording a calibration curve in buffer solution containing different amounts of dissolved hydrogen. The measured amperometric current of the micro-hydrogen biosensor was increasing with the hydrogen concentration from 1.6 µM to 32.5 µM (Fig. 4). At this low concentration of hydrogen a good linearity of the sensor response was obtained between 1.6 µM and 24 µM ($i_{(nA)}=(0.84 \pm 0.04)\times[H_2]_{(\mu M)} - (1.4 \pm 0.5)$; confidence intervals calculated for $\alpha=0.05$; $R^2=0.997$). The limit of detection (LOD)

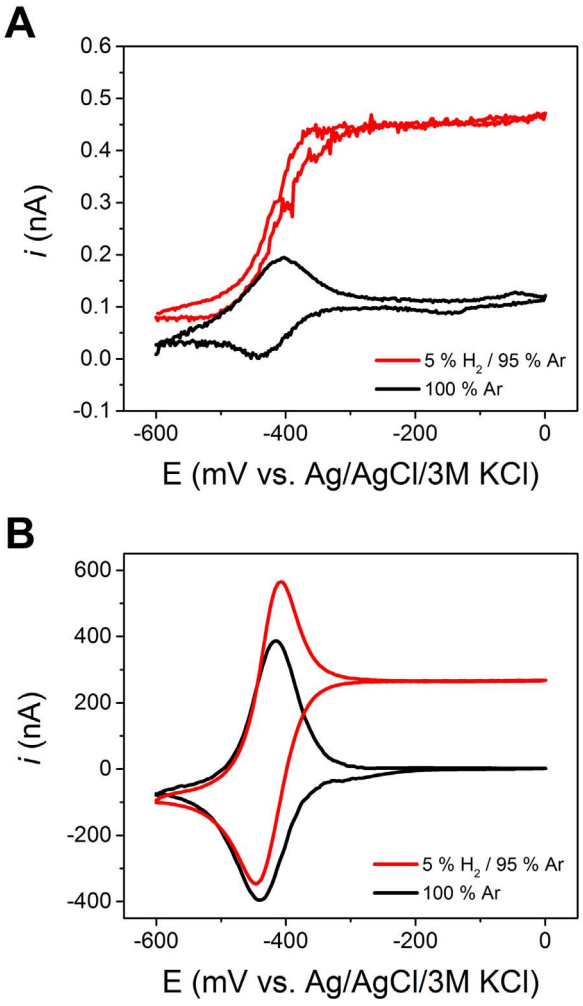

Fig. 3. Responses obtained for *Dv*MF [NiFe]-H_2ase/viologen polymer modified microelectrodes of different sizes. A) carbon fiber microelectrode with a diameter of ca. 7 µm; and B) carbon paste-based microelectrode with a diameter of 50 µm. Cyclic voltammograms were recorded in the presence and absence of H_2. Electrolyte: 0.1 M phosphate buffer, pH 7.0. Scan rate: 10 mV s^{-1}.

was calculated according to the $3 \cdot s_b/m$ criterion, where s_b is the standard deviation (n=10) of the blank response and m is the slope of the calibration curve. The calculated LOD was (0.81 ± 0.16) µM.

3.2. Analysis of a photosystem 1/Pt-based photocathode for hydrogen evolution

In order to demonstrate the capability of the fabricated micro-biosensor for local detection of hydrogen evolved at (bio)photocatalytically active samples, a PS1-Pt sample was selected. As described previously (Zhao et al., 2015), PS1-Pt bioconjugates embedded in an Os-complex modified redox polymer are capable of catalyzing the HER under irradiation. Upon absorption of photons of a suitable wavelength, charge-separation occurs in the PS1 protein complex. While the electrode surface serves as electron donor for delivering electrons to the P_{700}^+ site through the Os-complex modified redox polymer matrix, the high-energy electron at the F_B^- site of PS1 is transferred to the Pt nanoparticle for the reduction of protons in solution.

Photoinduced production of hydrogen was carried out at pH 4.0 in argon-saturated solutions. The rate of light-induced hydrogen evolution at the PS1-Pt biocomplexes embedded in the Os-complex modified hydrogel is dependent on the pH value and decreases with increasing pH value. In contrast, the catalytic activity of the [NiFe]-H_2ase/viologen polymer modified electrode is maximal at neutral pH value.

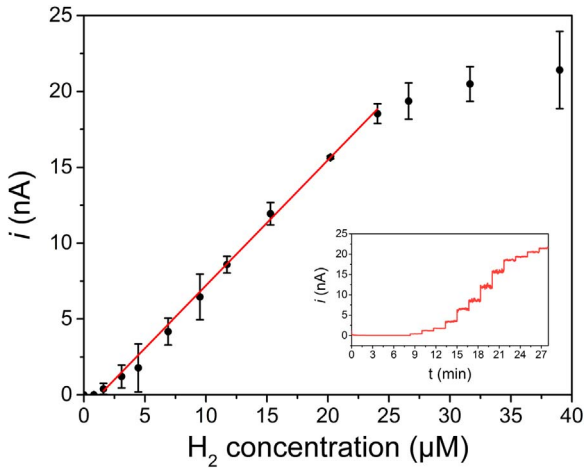

Fig. 4. Calibration curve obtained for *Dv*MF [NiFe]-H_2ase/viologen polymer modified microelectrodes (n=3) at different H_2 concentrations in 0.1 M phosphate buffer. The linear range is indicated by the red line. Error bars represent the standard deviation for the measurements. Inset: chronoamperometric response for a representative microbiosensor. E_{app}=0 mV (vs. Ag/AgCl/3 M KCl).

Therefore, an optimization of the measurement conditions is required, ensuring that the evolved hydrogen is detectable with the H_2ase-based micro-biosensor. For this, H_2ase/viologen polymer-modified electrodes were tested at different pH values. As shown in Fig. 5 the catalytic activity of the H_2ase-modified electrode decreases with decreasing pH value. Below pH 5.0 the catalytic activity decreases sharply and at pH 4.0 the response is negligible (data not shown) since at this pH value the redox potential of the $H_2/2H^+$ couple is already above the potential for the $V^{2+}/V^{+\bullet}$ redox couple in the polymer (Plumeré et al., 2014). In addition, as previously reported for the PS1-Pt complexes embedded in the Os-complex modified redox hydrogel, the current density obtained under irradiation which is directly related to hydrogen production, decreases sharply for pH values higher than 4.0 and is negligible above pH 6.0 (Zhao et al., 2015). Thus, the capability for sensitive hydrogen collection with the micro-biosensor was optimal at pH 5.0.

3.3. Scanning photoelectrochemical microscopy experiments

The hydrogen micro-biosensor was integrated into a scanning photoelectrochemical microscope (SPECM) and was used as local light source for the focalized irradiation of the sample and at the same time as a sensitive biosensor for hydrogen detection. By sensing variations in the rate of hydrogen evolution due to biocatalytic hydrogen oxidation, variations in PS1-Pt surface reactivity as a function of the probe location can be revealed. As proved experimentally (data not shown),

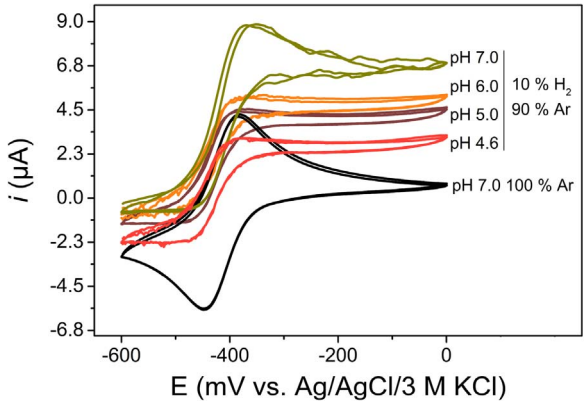

Fig. 5. Comparison of cyclic voltammograms for a *Dv*MF [NiFe]-H_2ase/viologen polymer modified glassy carbon electrode recorded in the presence and absence of H_2 at different pH values in 0.1 M phosphate buffer. Scan rate: 10 mV s^{-1}.

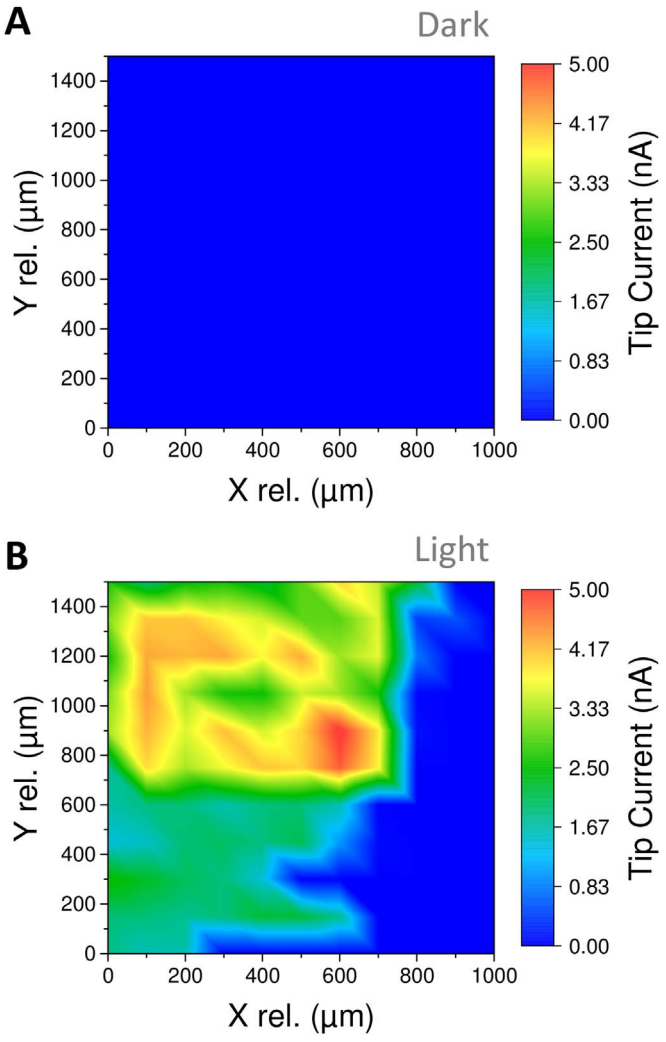

Fig. 6. SPECM scans of a spot of PS1-Pt/Os-complex-modified redox hydrogel partially covering the Au sample surface showing the current recorded at the tip by the *Dv*MF [NiFe]-H_2ase/viologen polymer modified microbiosensor: A) in the dark, B) under localized illumination of the sample through the positioned microbiosensor. E_{sample}=0 mV, E_{tip}=0 mV (both vs. Ag/AgCl/3 M KCl). Electrolyte solution: Ar-saturated phosphate-citrate buffer, pH 5.0.

the evaluated photocathode was stable under the experimental conditions for a period of time long enough to perform the SPECM scan.

An SPECM area scan above a PS1-Pt/Os-complex modified redox hydrogel sample was performed in buffer solution at pH 5.0 (Fig. 6) by moving the micro-biosensor both in *x* and *y* directions at a predefined tip-to-sample distance simultaneously automatically correcting for any surface tilt. While in the dark no significant oxidation current was detected (Fig. 6A), light-induced hydrogen evolution at the PS1-Pt modified sample was detected (Fig. 6B). Higher oxidation currents were observed with the microbiosensor positioned above regions of the sample modified with PS1-Pt. A clear contrast with the unmodified sample area was observed.

In comparison with a bare Pt microelectrode used for the visualization of the local hydrogen generation by PS1-Pt (Zhao et al., 2015), the tip current obtained with the hydrogenase-modified micro-biosensor is about 30-fold higher. In addition, a lower background current was registered in the dark, confirming the improved selectivity of the developed microbiosensor.

4. Conclusions

A versatile micro-biosensor was fabricated by modification of carbon-based microelectrodes with [NiFe]-H_2ase embedded in a viologen-modified redox hydrogel. The micro-biosensor is capable of the detection of hydrogen in solution with a remarkably high sensitivity. Future work is aiming on the integration of even more sensitive hydrogenases embedded in specifically adapted redox hydrogels. In combination with SPECM, the micro-biosensor was used for detection of locally evolved hydrogen and simultaneously for local illumination of the sample. Variations in the reactivity of a PS1-Pt sample towards hydrogen evolution were assessed providing simultaneous information about the photoelectrochemical properties of the sample and the collection of evolved reaction products.

Acknowledgments

The authors are grateful to P. Malkowski (MPI for Chemical Energy Conversion, Mülheim) for the isolation and purification of the *Dv*MF [NiFe]-hydrogenase and to C. König and M. Völkel for the preparation of PS1. This work was supported by the Cluster of Excellence RESOLV (EXC 1069) funded by the Deutsche Forschungsgemeinschaft (DFG), the Deutsch-Israelische Projektkooperation (DIP) in the framework of the project “Nanoengineered Optobioelectronics with Biomaterials and Bioinspired Assemblies”, and the ANR-DFG funded project “Shields” (PL 746/2-1). F. Z. and H. L. are grateful for the financial support by the China Scholarship Council (CSC).

References

Amemiya, S., Bard, A.J., Fan, F.-R.F., Mirkin, M.V., Unwin, P.R., 2008. Annu. Rev. Anal. Chem. 1, 95–131.
Badura, A., Guschin, D., Esper, B., Kothe, T., Neugebauer, S., Schuhmann, W., Rögner, M., 2008. Electroanalysis 20, 1043–1047.
Badura, A., Guschin, D., Kothe, T., Kopczak, M.J., Schuhmann, W., Rögner, M., 2011. Energy Environ. Sci. 4, 2435–2440.
Bertoncello, P., 2010. Energy Environ. Sci. 3, 1620–1633.
Cannan, S., Cervera, J., Steliaros, R.J., Bitziou, E., Whitworth, A.L., Unwin, P.R., 2011. Phys. Chem. Chem. Phys. 13, 5403–5412.
Clausmeyer, J., Actis, P., López Córdoba, A., Korchev, Y., Schuhmann, W., 2014. Electrochem. Commun. 40, 28–30.
Conzuelo, F., Sliozberg, K., Gutkowski, R., Grützke, S., Nebel, M., Schuhmann, W., 2017. Anal. Chem. 89, 1222–1228.
Edwards, M.A., Martin, S., Whitworth, A.L., Macpherson, J.V., Unwin, P.R., 2006. Physiol. Meas. 27, R63–R108.
Fichtner, C., Laurich, C., Bothe, E., Lubitz, W., 2006. Biochemistry 45, 9706–9716.
Fourmond, V., Stapf, S., Li, H., Buesen, D., Birrell, J., Rüdiger, O., Lubitz, W., Schuhmann, W., Plumeré, N., Léger, C., 2015. J. Am. Chem. Soc. 137, 5494–5505.
Jamali, S.S., Moulton, S.E., Tallman, D.E., Weber, J., Wallace, G.G., 2015. Surf. Interface Anal. 47, 1187–1191.
Jedraszko, J., Nogala, W., Adamiak, W., Girault, H.H., Opallo, M., 2014. Electrochem. Commun. 43, 22–24.
Kothe, T., Pöller, S., Zhao, F., Fortgang, P., Rögner, M., Schuhmann, W., Plumeré, N., 2014. Chem. Eur. J. 20, 11029–11034.
Krassen, H., Ott, S., Heberle, J., 2011. Phys. Chem. Chem. Phys. 13, 47–57.
Lubitz, W., Ogata, H., Rüdiger, O., Reijerse, E., 2014. Hydrog. Chem. Rev. 114, 4081–4148.
Oughli, A.A., Conzuelo, F., Winkler, M., Happe, T., Lubitz, W., Schuhmann, W., Rüdiger, O., Plumeré, N., 2015. Angew. Chem. Int. Ed. 54, 12329–12333.
Plumeré, N., Rüdiger, O., Oughli, A.A., Williams, R., Vivekananthan, J., Pöller, S., Schuhmann, W., Lubitz, W., 2014. Nat. Chem. 6, 822–827.
Reisner, E., 2011. Eur. J. Inorg. Chem. 2011, 1005–1016.
Sassolas, A., Blum, L.J., Leca-Bouvier, B.D., 2012. Biotechnol. Adv. 30, 489–511.
Schulte, A., Chow, R.H., 1996. Anal. Chem. 68, 3054–3058.
Sokol, K.P., Mersch, D., Hartmann, V., Zhang, J.Z., Nowaczyk, M.M., Rögner, M., Ruff, A., Schuhmann, W., Plumeré, N., Reisner, E., 2016. Energy Environ. Sci. 9, 3698–3709.
Sun, P., Laforge, F.O., Mirkin, M.V., 2007. Phys. Chem. Chem. Phys. 9, 802–823.
Tefashe, U.M., Snowden, M.E., Ducharme, P.D., Danaie, M., Botton, G.A., Mauzeroll, J., 2014. J. Electroanal. Chem. 720–721, 121–127.
Vesborg, P.C.K., Seger, B., Chorkendorff, I., 2015. J. Phys. Chem. Lett. 6, 951–957.
Yagi, T., Kimura, K., Daidoji, H., Sakai, F., Tamura, S., 1976. J. Biochem. 79, 661–671.
Zhao, F., Conzuelo, F., Hartmann, V., Li, H., Nowaczyk, M.M., Plumeré, N., Rögner, M., Schuhmann, W., 2015. J. Phys. Chem. B 119, 13726–13731.
Zheng, Y., Jiao, Y., Zhu, Y., Li, L.H., Han, Y., Chen, Y., Du, A., Jaroniec, M., Qiao, S.Z., 2014. Nat. Commun. 5, 3783.
Zoski, C.G., 2015. Electrochem. Soc. 163, H3088–H3100.